Quantification of larval traits driving connectivity: the case of Corallium rubrum (L. 1758)

A. Martínez-Quintana, L. Bramanti, N. Viladrich, S. Rossi, Katell Guizien

Quantification of larval traits driving connectivity: the case of *Corallium rubrum* (L. 1758)

A. Martínez-Quintana[1], L. Bramanti[1,2*], N. Viladrich[3], S. Rossi[3,4], K. Guizien[2]

[1] Institut de Ciències del Mar, ICM-CSIC, Passeig Marítim de la Barceloneta, 37-49, 08003 Barcelona (SPAIN)

[2] Laboratoire d'Ecogéochimie des Environnements Benthiques, CNRS-UPMC, Observatoire Océanologique de Banyuls sur Mer, Avenue du Fontaulé - 66650 Banyuls sur Mer (FRANCE)

[3] Institute of Environmental Science and Technology (ICTA), Universitat Autònoma de Barcelona (UAB), Building C Campus UAB, 08193 Bellaterra (Cerdanyola del Vallès), Barcelona (SPAIN)

[4] Unidad de sistemas Arrecifales, Instituto de Ciencias del Mar y Limnología, Universidad Nacional Autónoma de México, CP 77500, Cancún(MEXICO)

Keywords: Red coral; Metapopulation; Motility behavior; Larval dispersal; Conservation spatial planning; Pelagic larval duration

Corresponding Author: Lorenzo Bramanti

Current address: CNRS, Université Pierre et Marie Curie, UMR8222, LECOB, Observatoire Océanologique, Avenue du Fontaulé, 66650, Banyuls/mer, France

Email: philebo@gmail.com

Tel. +33 468887319

Abstract

Larval dispersal is the process enabling connectivity between populations of marine species with a sedentary adult stage. This transportation results from the coupling between flow and larval biological traits. This experimental study aims to quantify these larval biological traits, namely pelagic larval duration (PLD), buoyancy, and larval vertical motility behavior, for *Corallium rubrum*. Larval vertical motility behavior was split into active behavior (swimming) and passive behavior (free fall). A particle tracking routine was applied to video recordings of the active and passive motility behavior of *C. rubrum* larvae to quantify their free fall speeds, swimming activity frequency, and swimming speeds. The experiment was repeated under different light conditions and at different larval ages. Pelagic larval duration (PLD) ranged from 16 days (95% survival) to 42 days (5% survival). Larvae exhibited negative buoyancy with a free fall speed decreasing linearly with age, at a velocity varying from -0.09 ± 0.026 cm s^{-1} on day 1, to -0.05 ± 0.026 cm s^{-1} on day 10. No significant difference was found either in the activity frequency or in the mean swim velocities during active periods for age (up to 12 days old) or under different light conditions. *C. rubrum* larvae maintained active swimming behavior for 82% of the time. This activity frequency was combined with age-varying free fall periods in the motility behavior model extrapolated up to 15 days old, resulting in a mean upward speed that increased from 0.045 cm s^{-1} (day 1) to 0.056 cm s^{-1} (day 15). This larval motility behavior, combined with the extended PLD, confers on *C. rubrum* larvae an unexpectedly high dispersive potential in open waters.

1. Introduction

Most marine benthic invertebrates release larvae and/or gametes (Thorson 1946) that are advected and dispersed by ocean currents before becoming competent to settle in a suitable place. Larval dispersal is the process enabling connectivity within a marine metapopulation, and has been highlighted as a key mechanism for population recovery after local extirpation from specific areas (Lipcius et al. 2008). It is thus considered crucial in the development of conservation strategies and in the design of marine protected areas (MPA) (Shanks et al. 2003; Guizien et al. 2014). Direct measurement of the magnitude of this dispersal should involve tracking individuals from a release site to settlement. Tracking techniques have been used with success on large organisms such as fishes (Planes et al. 2009), but are still difficult to apply in the case of small-sized benthic invertebrates with long pelagic larval duration (PLD; Levin 1990). Therefore, the quantification of dispersal distances using direct field observations has been possible only for those species characterized by large-sized larvae with short PLD (e.g., tunicates; Bingham and Young 1991; Queiroga and Blanton 2004). Indirect methods are based on the assumption that larval dispersal maintains genetic continuity and gene flow among populations (Palumbi 2003; Levin 2006). Another indirect approach to larval dispersal is the integration of larval motility behavior along the PLD with physical processes of 3D advection and diffusion caused by currents (Levin 2006; Cowen and Sponaugle 2009). Lagrangian tracking numerical models integrating flow conditions over the PLD are frequently used to forecast larval dispersal patterns (e.g., Lett et al. 2008; Paris et al. 2013), generally neglecting larval behavior (but see Guizien et al., 2006). However, small vertical velocities, as displayed by most marine benthic

invertebrate larvae (Chia et al. 1984), could affect their horizontal dispersal in a non-vertically homogeneous flow field (e.g., Mileikovsky 1973; Queiroga and Blanton 2004).

The Mediterranean red coral (*Corallium rubrum*, L. 1758) is a gonochoric long-lived octocoral endemic to the Mediterranean Sea and its neighboring Atlantic rocky shores, where it can be found at depths between 10 and 800 m (Costantini et al. 2010). *C. rubrum* is currently listed among the species of community interest in the European Union Habitat Directive (92/43/EEC, Appendix V) given its ecological, economical and patrimonial value (sensu Bramanti et al. 2011). This engineering species contributes to the biomass and energy flow of the Mediterranean rocky bottom communities (Gili and Coma 1998), and changes in its abundance and population structure could affect the whole community (Garrabou and Harmelin 2002). Harvested and traded since antiquity due to its calcareous axial skeleton used as raw material for jewelry, red coral is an example of long-lasting harvesting pressure focused on a single species (Tsounis et al. 2010). Local demographic population models have been developed to project the shallow population structure of *C. rubrum* over time under different scenarios (e.g., overexploitation and thermal stress), and to provide advice concerning conservation and management (Bramanti et al. 2009, 2014). Coral populations live in a fragmented seascape in which connectivity arising from larval dispersal can influence local population resilience (Cowen et al. 2000; Jones et al. 2007). Assessing the recovery potential of *C. rubrum* shallow populations through connectivity with deep populations or protected shallow ones is particularly important given the massive demographic disturbances affecting shallow populations of this species (Linares et al. 2012). Like most cnidarians, *C. rubrum* releases lecithotrophic, aposymbiotic ciliated larvae (planulae), which are

white and club-shaped with a major axis of ~1 mm and a minor axis of 0.3 mm. Planulae are internally brooded and released once a year over a period of approximately two weeks between the end of July and early August (Santangelo et al. 2003; Bramanti et al. 2005). The strong differentiation in allele frequencies at short distances within *C. rubrum* populations (Costantini et al. 2007, Ledoux et al. 2010) suggests a low dispersive potential in planulae, resulting in high larval retention around parental colonies. This low dispersive potential has been attributed to the brief PLD of 4–12 days observed by Vighi (1972), although the PLD alone may not be sufficient to estimate dispersal distances (Kelly and Palumbi 2010).

In this study, to enable species-dedicated connectivity estimates of *Corallium rubrum* based on larval dispersal simulations, survival and motility behavior were studied experimentally during the larval phase. PLD, buoyancy, free fall speed, swimming activity frequency (percentage of time during which active swimming behavior is displayed), and swimming velocities of *C. rubrum* larvae were quantified. Larval traits were then assembled to develop a synthetic model of the larval motility behavior in the form of cumulative velocity distributions (CFD, Fig. S1, Online Material 1); this model is applied to perform larval dispersal simulations.

2. Materials and Methods

2.1 Larvae collection

Colonies were collected at a depth of 25–30 m on a coralligenous habitat (42º 26.885' N, 03º 10.368' E, Banyuls-sur-Mer, NW Mediterranean Sea, France).

The larvae used in the motility experiment were obtained from 12 *C. rubrum* female colonies with basal diameters larger than 7 mm and heights of 60–120 mm. These colonies were collected in late July 2012. For the PLD assessment, 12 additional female colonies were collected in late July 2013. For complementary free fall measurements, 10 additional female colonies were collected in July 2014. All colonies were transferred to closed aquaria at 16–17 ºC (temperature measured *in situ*) just before larval release.

For the motility experiment, planulae released over a seven-day period (July 28 to August 3, 2012) were subdivided into 0.4 L glass containers with filtered seawater (< 5 µm) according to the date of their release. The same procedure was applied in 2014 for complementary free fall measurements using larvae released over seven days (July 21 to 28, 2014). For PLD assessment, larvae released over six days (July 25 to July 30, 2013) were separated into three release events of two consecutive days each (T1, T2, and T3). This procedure was adopted to test the effect of within-brood variability (larval size or energy reserve) on PLD. For each release event, 390 larvae were chosen at random and subdivided into three 0.4 L glass containers (replicates, n = 130) with filtered seawater (5 µm). The filtered seawater was renewed daily and larvae were kept in darkness at a temperature of 19–21 ºC, which is the vertically averaged temperature in late July–August over a 27 m water depth in Banyuls sur mer Bay (Service d'Observation du Laboratoire Arago).

2.3 Pelagic larval duration and larval mortality rates

To quantify PLD and daily mortality rates, larval counts were performed every other day (precision of 3%, estimated from repeated counts). For each

release event (n = 3), minimum, median and maximum PLD were defined as the time from larval release at which 5%, 50% and 95% of the initial number of larvae had died. A one-way ANOVA (R command “aov,” package “stats,” R Core Team, 2014) was performed to test the effect of the factor “Release event” (three levels, T1, T2, and T3, and three replicates for each level) on minimum, median and maximum PLD. When a difference was detected, a post hoc test was performed (R command “TukeyHSD,” package “stats,” R Core Team, 2014). Mean daily mortality percentages were calculated during minimum PLD, between minimum and median PLD, and between median and maximum PLD. A one-way ANOVA was performed to test the effect of larval age (three levels corresponding to the three periods defined above, three replicates for each level) on mortality. When a difference was detected, post hoc tests were performed.

2.4 Body density and free fall speed of inactive larvae

The buoyancy of planulae is defined by the difference in body density relative to the seawater density. It may be positive, negative or neutral and determines sinking or floating behavior during periods of inactivity at sea. In this study, a modified dual-density method (Pennington and Emlet, 1986) was used to estimate the specific body density of planulae by observing whether they floated or sank through a series of eight density gradients produced by layering seawater at 20 °C (density of 1.027 g ml^{-1}) over a sucrose solution (distilled water plus sucrose) with densities ranging from 1.03 to 1.08 g ml^{-1}. A tube with seawater at 20 °C was used to test positive buoyancy.

Larvae were anesthetized by exposing them for 15 min in 10 ml of seawater with two drops of either eugenol (clove oil, immiscible, density 1.06 mg

l^{-1}) or menthol (mint oil, density 0.89 mg l^{-1}). Anesthesia was done by oil vapor inside a Petri dish avoiding the direct contact of larvae with the oil. This procedure was followed to immobilize the larvae without killing them, maintaining their shape and thus their hydrodynamic properties. Anesthetized larvae were checked under a stereomicroscope and those with visible damage or that had died were rejected. Between 8 and 10 larvae anesthetized with eugenol were injected sequentially in each test tube and were allowed to settle for 15 minutes into the density gradient produced by the two fluids. Only the larvae that sank to the bottom were considered denser than the corresponding sucrose solution. This procedure was carried out every day during the period of PLD (15 days), during which mortality losses can be discounted (less than 5%). A cumulative frequency distribution of body densities was built for each day, reporting the percentage of larvae denser than each sucrose solution (n = 8–10 larvae). The 20% and 80% quantiles of these cumulative frequency distributions were used to define the range of larval body density values. Large inter-individual variability resulted in non-monotonous larval body density frequency distribution on four days (out of 15) given the small number of larvae assayed (n = 10). Therefore, it was not possible to define the 20% and 80% quantiles for those days.

Free fall experiments were carried out for larvae aged 1, 4, 8, and 10 days. For each larval age, two groups of at least 10 larvae were anesthetized with eugenol (group 1) and menthol (group 2) and gently injected into a wide container (10 cm diameter, 14 cm height) one by one to minimize the movement caused by the injection itself. A free fall time over a height of 9 cm was used to calculate the free fall speed of individual larvae. The correlation between age and sink speed was tested. If the correlation was significant, the null slope of the linear regression was tested to assess the presence of a trend in the larval fall speed during the first

10 days for the two groups, and significant differences between linear regression fit for groups 1 and 2 were tested. An 80% confidence interval around the linear regression slope estimates was also calculated.

2.5 Larval active motility behavior: Swimming activity frequency and speeds of active larvae

Larval active motility behavior (swimming activity frequency and swimming velocities CFD of active larvae; for further detail, see Online Material 1) was quantified for a group of 30 larvae randomly chosen each day during the first 15 days of PLD (except on day 14 for which data were missing). In the case of benthic invertebrates with horizontal swimming velocities lower than 1 cm s^{-1}, such quantifications can be restricted to vertical motility behavior.

Vertical motility behavior measurements were carried out in transparent, flat-faced plastic containers of 50 ml (38 × 60 × 20 mm). The 30 larvae were divided into two groups (n = 15 each) and injected into two different containers to avoid interference due to overcrowding. The two containers, being assayed simultaneously, were treated as replicates. A small distance between the front and back walls (20 mm) of containers was chosen: 1) to constrain larvae in the vertical motion, and 2) to maintain them in the focal plan of the camera in order to avoid losing track of individuals, thus ensuring automated particle tracking with 100% restitution. Larval active motility behavior was recorded at 25 frames per second with a digital camera (SONY DCR-SR78); films were sub-sampled into a sequence of frames taken at a rate of 0.5 s. Larval vertical velocities (positive upward) were calculated from film-extracted tracks reconstructed using a particle-tracking routine developed by the authors using the Matlab Image Processing

toolbox (for further detail, see Online Material 2). Due to the limited size of the containers, velocity measurements could have been underestimated due to “wall effects” creating additional drag at low Reynolds numbers (Vogel 1994). The distance to the nearest wall is of major concern in determining the free fall speed because the laminar boundary layer extends to at least 100 times the equivalent radius of the larvae. However, the distance to the nearest wall is less crucial during active swimming behavior when intermittent propulsion drastically decreases the thickness of the boundary layer around the larva by at least a factor of 10 (Winet 1973). To detect periods in which larvae were free falling along active tracks, *ad hoc* free fall experiments in the same flat-faced plastic containers were performed and free fall speeds of confined larvae were determined (see Online Material 3).

During each daily experiment, larvae were exposed alternately to cold white light (CWL, 6500 K, PAR = 480 µmol photons m^{-2} s^{-1}) and to infrared (IR) light (PAR < 1 µmol photons m^{-2} s^{-1}) during six successive sequences of 15 min long. Recording started two minutes after injection of the last larva, ensuring any flow motion due to injection had disappeared when recording started. Kinesthetic stimulation was obtained by injecting water into the container in which the larvae were stored using a pipette just before transferring them to the small experimental container. To obtain approximately the same level of kinesthetic stimulation for all the replicates, a similar number of pipette injections were applied each time. The effect of such stimulation was assumed to decay during the experiment. We evaluated separately the effect on activity frequency of 1) kinesthetic stimulation, 2) age, and 3) light conditions in the absence of kinesthetic stimulation (Guizien et al. 2006).

Inactive periods were detected as the time during which larvae were either free falling or remained at the bottom of containers (see Online Material 1). Not

anesthetized larvae were considered as freely falling when larvae speed was equal to any of the free fall speeds measured on anesthetized larvae in the vials (see Online Material 3), since the position of the larvae with respect to the nearest wall could not be known.

Activity frequency was calculated for each of the two groups of 15 larvae (replicates, n = 2) and for each 15 min long sequence. First the effect of the kinesthetic stimulation was tested by applying a paired t-test to compare every day (n = 14) activity frequency during the first 15 min of CWL (CWL1, less than 10 min after kinesthetic stimulation was stopped) to activity frequency during the last 15 min of CWL (CWL3, more than 1 h after kinesthetic stimulation was stopped). To test if the kinesthetic stimulation effect disappeared after 30 min, two paired t-tests were applied comparing every day (n = 14) activity frequency during the first and second 15 min slots of CWL (CWL1 versus CWL2), and during the second and third 15 min slots (CWL2 versus CWL3).

Once it had been verified that an effect of kinesthetic stimulation exists and disappears after 30 min, another paired t-test comparing the recordings under CWL conditions and IR conditions after 30 min was performed to test the effect of light exposure on activity frequency.

Finally, the existence of a trend in activity frequency during the first 15 days was assessed by testing the correlation between age and activity frequency. Vertical velocity components were calculated from larval tracks and filtered out by eliminating unrealistic acceleration due to the injection (> 1.5 cm s^{-1}). The larval active swimming motion was described as random behavior inside the vials (see Online Material 1), and frequency distributions of net swimming velocities (removing velocities in the range of free fall velocities) for each sequence of recording 15 min long under different light exposures were built. As differences in

the cumulative swimming velocity distributions under CWL (excluding the first 15 min) and IR exposure were lower than the measurement resolution (0.016 cm s^{-1}), the effect of light could be discounted compared to the effect of the kinesthetic stimulation, and only the swimming velocities measured during the first 15 min of recording were taken into account.

To assess the existence of a trend in the average net swim velocity during the first 12 days, the correlation between age and average swim velocity (average larval velocity CFD after discarding free falling velocities along larval tracks) was tested.

3. Results

3.1 Mortality rates and duration of pelagic larval stage from laboratory experiments

On average, the minimum PLD was 16.2 ± 1.9 days, the median PLD was 28.9 ± 3.3 days, and the maximum PLD was 41.7 ± 4.9 days, without differentiating release events. No significant differences between the three larval release events were found in minimum PLD (ANOVA: $F_{2,6} = 2.2$, $p > 0.5$), while median PLD significantly increased from the first release event to the third with values of 25.3, 28.7, and 32.7 days, respectively (ANOVA: $F_{2,6} = 30.3$, $p < 0.001$; TukeyHSD: T1 < T2 < T3). Maximum PLD did not differ significantly between release events 1 and 2 (39 days), while it was significantly greater (47 days) for the third event (ANOVA: $F_{2,6} = 6.3$, $p < 0.05$; TukeyHSD: T1 = T2 < T3). Daily mortality percentages increased significantly with larval age (ANOVA: $F_{2,18} = 18.24$; $p < 0.001$), with values of mean ± SD = 0.3% ± 0.004% d^{-1} during

minimum PLD, 5.8% ± 2.4% d^{-1} between minimum and median PLD, and 21.5% ± 13.81% d^{-1} between median and maximum PLD.

3.2 Larval body density and free fall velocities

All anesthetized larvae injected in seawater solutions showed negative buoyancy during the experiment, with 80% still exhibiting a density greater than 1.027 g ml^{-1} at day 15. Despite the considerable uncertainties due to the limited number of larvae assayed (10 larvae per sucrose solution density tested), the changes in the buoyancy thresholds suggest that larval body density decreases with age (Fig. 1A). The larval free fall velocities increased significantly with age whatever the anesthetic treatment (t-test: p value < 0.01; R^2 = 0.27 for eugenol and R^2= 0.09 for menthol), and linear regression fits were not significantly different (Fisher-Snedecor test of variance: $F_{78,72}$ = 1.2, p > 0.05 ; t-test of slope: t_{150} = 2 10^{-6}, p > 0.9; t-test of intercept: t_{150} = 6.8 10^{-5}, p > 0.9). Thus, free fall velocities during passive phases were modeled by a normal distribution, with mean ± SD (defined by the 80% confidence interval, Fig. 1B) varying linearly from -0.09 ± 0.026 cm s^{-1} on day 1 to -0.05 ± 0.026 cm s^{-1} on day 10, which was extrapolated to -0.03 ± 0.026 cm s^{-1} on day 15.

3.3 Swimming activity frequency

C. rubrum larvae are active swimmers, spending less than 25% of the time at the bottom of the containers over the duration of the recording period (554 h). Moreover, the larval activity frequency was significantly higher during the first slot of 15 min (CWL1) of each day compared to the second (CWL2) and third

(CWL3) slots of 15 min under CWL conditions (paired t-test: CWL1 vs CWL2: $t_{12} = 6.54$, $p < 0.05$; CWL1 vs CWL3: $t_{12} = 5.26$, $p < 0.05$). The effect of kinesthetic stimulation ended after 30 min as no significant difference was found between CWL2 and CWL3 (paired t-test: $t_{12} = 0.68$, $p > 0.05$). In addition, no significant difference was found between activity frequencies in consecutive 15 min slots with different light conditions (paired t-test: $t_{12} = 0.89$, $p > 0.05$).

The decay observed in activity frequency during the experiments was attributed to a decrease in the effect of kinesthetic stimulation due to larval manipulation before the beginning of the experiment (see 2.5). Assuming such stimulation would be frequent in the natural environment because of sea turbulence, only swimming activity frequencies during the first 15 min under CWL conditions were subject to further analysis (Fig. 2). No significant correlation between age and activity frequency was observed during the first 15 days (t-test: $R^2 = 0.09$, $p > 0.1$).

The average swimming activity frequency during the first 15 days of PLD was 82% ± 14.5% (mean ± SD) with larvae at the free water surface 73% of the time and in the water column 9% of the time. If restricted to larvae in the water column, swimming activity frequency (larval velocities different from free fall velocities) yielded 76% ± 17% (mean ± SD).

3.4 Swimming velocity measurements

The velocities of *C. rubrum* larvae along tracks varied between -0.1 cm s^{-1} and 0.2 cm s^{-1} (Fig. 3). Larvae exhibited a clear upward swimming behavior. Downward speeds (negative velocities) were in the range of uncorrected free fall speed (-0.1 cm s^{-1} to -0.04 cm s^{-1}, Online Material 3) and represented between 7%

and 40% of time in these velocity distributions. They were removed from the velocity distribution to obtain net swim velocity distributions. No significant correlation between age and average net swim velocity (upward speed) of active larvae was observed during the first 12 days (t-test: $R^2 = 0.16$, $p > 0.05$).

Thus, the distribution of swim velocities of all larvae assayed (n = 336) were pooled to build a single swim velocity distribution (Fig. 3). This net swim velocity distribution was then combined (equation (1); Online Material 1) with the unbounded normally distributed free fall speed for each age (see above) to build a synthetic model for *C. rubrum* larval motility behavior in the first 15 days, i.e., the PLD period during which mortality was minimum (less than 5%).

The model is derived from measurements to day 10, and extrapolated up to day 15, projecting the linear regression of sinking speed measurements and assuming that swimming velocities and activity frequency remained unchanged after day 12 (assumption supported by the high swimming activity frequency measured on days 13 and 15, although not replicated). The extrapolation of sinking speed regression from day 10 to day 15 is supported by the fact that larval body density (Fig. 1A) and sinking speeds measured with wall effects from day 10 to day 15 consistently showed the same decreasing trend (Online Material 3).

This synthetic model is the weighted sum of:

1) The cumulative frequency distribution (CFD) of normally distributed free fall velocity for each age multiplied by 19.4% (proportion of experiment time that larvae spent at the bottom in the experimental device plus the proportion of experiment time larvae were free falling along tracks).
2) The CFD of net swim velocity (not free falling) distribution along tracks multiplied by 7.6% (proportion of experiment time that larvae were swimming along tracks).

3) The CFD of positive net swim velocity distribution along tracks multiplied by 73% (proportion of time that larvae spent at the free surface).

Fig. 4 shows the modeled CFD of net larvae velocities varying with larval age, as a result of the increase in free fall velocity mentioned earlier. In summary, the active swimming behavior overcame the passive free fall, resulting in a mean upward velocity that increased with larval age from 0.045 cm s^{-1} on day 1 to 0.056 cm s^{-1} on day 15.

4. Discussion

4.1 Larval traits driving connectivity

In this study, we quantified pelagic larval duration (PLD), daily mortality rates, buoyancy, and the motility capability of *C. rubrum* larvae. The data acquired were synthetized in a model for larval motility behavior, the results of which suggest a high dispersal potential in open water.

According to our results, *C. rubrum* larvae could survive at least 16 days (potentially up to 42 days) in plankton, with intrinsic daily mortality rates lower than 6% for 25 days after release. Also, not taking into account the maximum PLD of 42 days when only 5% of larvae survive, the values of the minimum and median PLD are higher than the 4–12 days previously reported by Vighi (1972) in similar conditions (without predation and other mortality sources). Such different PLD estimates could be due to the limited number of observations in the former study (n = 50) compared to this study (n = 1170), or to differences in temperature conditions (not specified in Vighi 1972).

Median and maximum PLD varies between larvae released on different days, supporting the hypothesis of a between-brood variability of survival expectancy. It is well established that the size of the eggs in scleractinian corals can vary within a brood (Sier and Olive 1994; Cumbo et al. 2012). In the case of lecitothrophic larvae, variable larval size results in differential energy reserves, and consequently larvae survival expectancy and PLD (Isomura and Nishishira 2001). According to bet-hedging theory (Stearns 1976; Seger and Brockmann 1987), organisms inhabiting highly variable environments increase their fitness by producing phenotypically diverse offspring (Crean and Marshall 2009). Studies on the energetic content of *C. rubrum* larvae released at different times are needed to investigate further the bet-hedging strategy in this species.

The values of PLD found in our study are comparable to those observed for other octocoral species with aposymbiotic larvae (Ben-David-Zaslow and Benayahu 1998; Harii et al. 2002), and for several benthic invertebrates in temperate waters (Mc Edward 1995; Shanks 2009). Studies on species with PLDs of three weeks have shown dispersal distances of several km (Moran et al. 1992; Schwindt 2007), suggesting that *C. rubrum* larvae in similar flow conditions could disperse the same distances. However, dispersal distances cannot be inferred solely from PLD; rather, integration between PLD and transport velocities is needed (Guizien et al. 2012).

Due to the limitations linked to laboratory experiments, which cannot take into account different sources of mortality present in the field (e.g., predation), our results for PLD represent the maximum intrinsic survival of the larvae. Notwithstanding these limits, such PLD, estimated in the absence of pressures, will allow first calculations of potential dispersal distances integrating PLD and transport velocities in sites where *C. rubrum* populations are present.

All anesthetized larvae showed negative buoyancy with free fall speeds of the same order of magnitude as those estimated for other benthic invertebrate larvae (Chia et al. 1984; Guizien et al. 2006). Lecithotrophic larvae consume energy reserves during development, leading to decreases in lipid content and changes in lipid composition (Harii et al. 2007), and this likely causes the decrease in larval body density and free fall speed with age observed in this study (Fig. 1). A decrease in the content of wax esters during PLD has been documented for broadcast-spawning and brooding corals (Harii et al. 2007; Figueiredo et al. 2012), and has been related to buoyancy decrease in PLD (Harii et al. 2007). Our results show an opposite trend that could be explained by a different composition of stored lipid in *C. rubrum* planulae, such as triacylglycerols, which are denser than seawater (Lee et al. 2006; Harii et al. 2007). The results of previous experiments showing an upward movement of *C. rubrum* larvae (Weinberg 1979) should then be interpreted as a consequence of active upward swimming behavior. Although surprising, high frequencies of activity are not uncommon in species with aposymbiotic lecitotrophic planula larvae (*Dendronephthya hemprichi*, Dahan and Benayahu 1998; *Acropora latistella*, *Montastraea magnistellata*, *Favia pallida*, *Goniastrea aspera* and *Pectinia paeonia*, Graham et al. 2013).

According to our results, light conditions do not affect activity frequency or swimming speed, confirming the lack of phototaxis of *C. rubrum* larvae observed by Weinberg (1979). In contrast, this study indicates that activity frequency increases after kinesthetic stimulation, as observed by Guizien et al. (2006) in the polychaete *Owenia fusiformis* larvae. However, given the simple procedure used to apply the kinesthetic stimulation, the quantification (or variation) of the turbulence level experienced by larvae was not possible in our study. As the response to mechanical stimulation could induce a bias in swimming

behavior experiments in the absence of flow (Pawlik and Butman 1993), behavioral studies performed in controlled flow facilities would give more realistic results (Wheeler et al. 2013). In this kind of approach, though, there are technical constraints in terms of the possibility of resolving the difference between flow and larval motion, and thus it can be applied only to larvae with high swimming speeds, unlike *C. rubrum* larvae with speeds of less than 0.26 $cm.s^{-1}$.

However, notwithstanding their slow swimming speed compared to other benthic invertebrate larvae (Chia et al. 1984), *C. rubrum* planulae show a high activity frequency resulting in a mean upward velocity that would maintain larvae in the water column. According to a raw estimate based on the average upward velocity, in the absence of vertical flow, larvae should move 61 cm vertically in the first hour after release and 38 m during the first 24 h. This movement should be enough to allow *C. rubrum* larvae to escape from the bottom boundary layer, where flow speed is lower, and disperse in the open water, as observed for other species (*Pocillopora.damicornis*, Harii et al. 2002; *Eunicella singularis*, Theodor 1967). However, it should be emphasized that such upward swimming could increase larval retention in the vault of crevices.

C. rubrum releases large lecitotrophic larvae (~ 1 mm long), with a fecundity that is low compared to other species with planktotrophic larvae within the same environment (~ 6500 larvae released by a 54-year-old *C. rubrum* colony versus 10^4 to 10^5 larvae $female^{-1}$ estimated for the polychaete *Ditrupa arietina*; Charles et al. 2003; Santangelo et al. 2007). The fitness maximization principle, when applied to large and not numerous larvae, suggests that larvae should display a low dispersive behavior (short PLD, low swimming ability) to reduce dispersal losses (Stearns 1992). Nevertheless, our results show that high activity

frequency and long PLD favor high dispersal potential, suggesting that fitness might be driven not only by dispersal risk but also by chances of survival. Indeed, due to the inverse relationship between prey size and predation risk (Cowan et al. 1996), the lower number of lecithotrophic larvae may not represent such a disadvantage, as losses during larval dispersal could be compensated by fewer losses due to predation compared to planktothrophic larvae (which could suffer additional loss due to starvation).

4.2 Implications for *C. rubrum* population connectivity

The active upward swimming behavior of *C. rubrum* larvae together with a minimum PLD of 16 days enhances the likelihood that a large percentage of the cohort will be transported away from their parental population after release. This should imply a low local retention when combined with flow motion, with the exception of caves and crevices in which local retention could be higher. According to Guizien et al. (2012), a species with neutrally buoyant larvae and PLD of two weeks would disperse over more than 10 km in the Gulf of Lions. Thus, *C. rubrum* planulae should disperse and promote connectivity between distant populations.

Such high dispersal ability is an apparent paradox, as previous studies on *C. rubrum* genotypic diversity have revealed a strong genetic structuring on small spatial scales, attributed to a limited dispersal capacity of larvae (Costantini et al. 2007; Ledoux et al. 2010). Genetic methods based on markers (e.g., mitochondrial DNA and microsatellites) provide insights into the spatial scales of existing long-term connectivity among multiple populations (Lowe and Allendorf 2010). Yet, genetic connectivity does not depend only on dispersal processes but also on

settlement, post recruitment survival, and successful mating in the next generations. A strong genetic structure also would arise when selective forces acting locally on recruitment and producing genetic drift (i.e., predation, availability of settlement habitat, and/or competition) overcome dispersal forces mixing populations at the regional level (Lowe and Allendorf 2010). Such strong selective forces are not unexpected in stable populations of a long-lived species such as *C. rubrum*, in which gene flow may be limited considerably by intra-specific density-dependent recruitment limitation (Santangelo et al. 2007), as well as strong sciaphilic habitat preferences in the shallow environment (Rossi et al. 2008). Conversely, in populations of long-lived species, mixing may be facilitated by the increased availability of suitable settlement habitats after mortality events (Arnold and Steneck, 2011). Thus, estimating the potential recovery of populations after demographic disturbances requires insights into potential connectivity through the larval dispersal phase of the species.

In conclusion, our results present strong evidence of a high dispersal capacity for *C. rubrum* larvae and hence of potential hydrodynamic connectivity between distant populations.

Figure

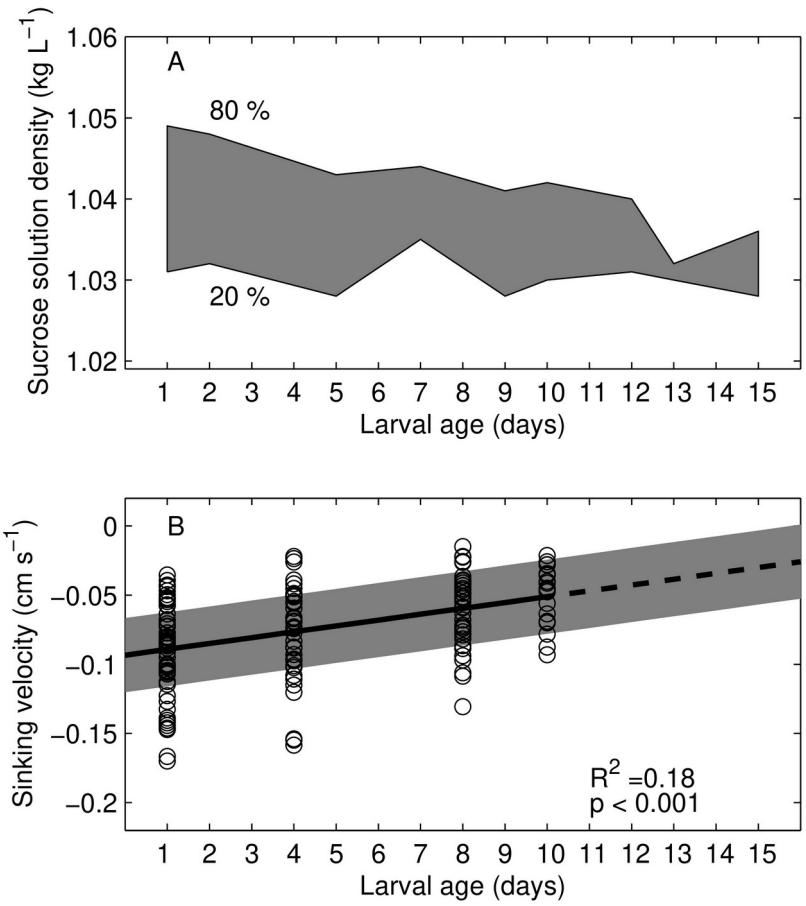

Fig. 1 (A) Larval body density of *Corallium rubrum* during the first 15 days of PLD. Values between the 80% and 20% quantiles displayed by the grey area. (B) Individual free fall velocities of *C. rubrum* larvae aged 1, 4, 8, and 10 days measured in a large container (hollow circles). Mean sinking velocity values (solid line) and 80% confidence intervals around the mean (grey area) estimated from linear regression.

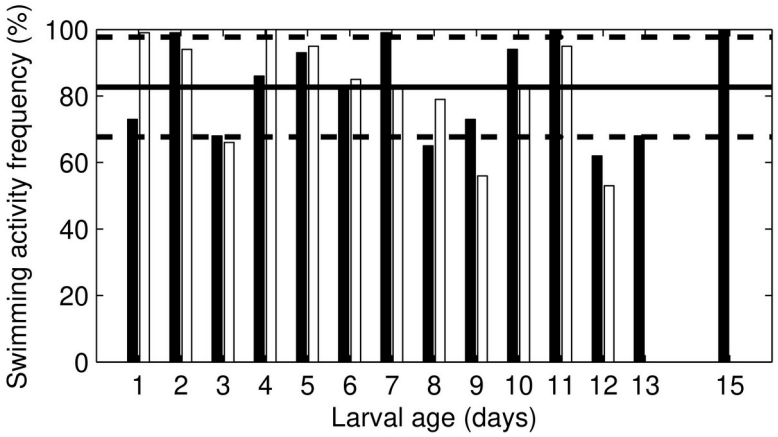

Fig. 2 Mean swimming activity frequency of two groups of 15 larvae (black and white bars) during the first 15 days of PLD with mean (solid line) and standard deviation (dashed lines).

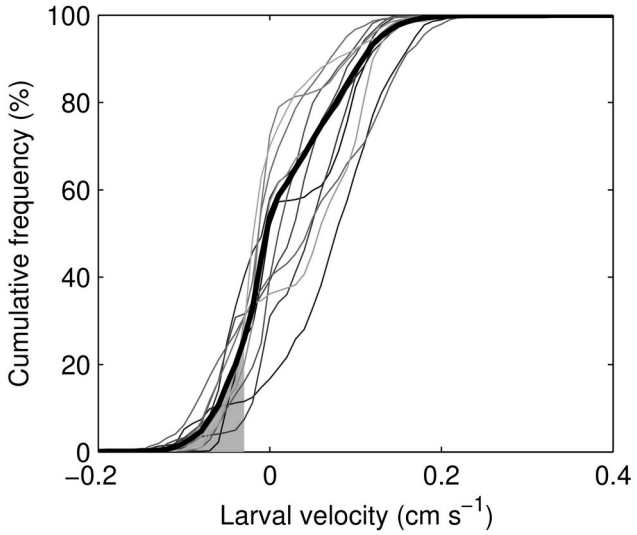

Fig. 3 Cumulative frequency distribution of measured swimming velocities for groups of 30 larvae at different ages ranging from one day old (darker gray) to 12 days old (lighter gray). The thick line displays the average CFD over the first 12 days, pooling measurements over 336 larvae. The grey area displays free fall velocities removed to obtain the CFD of swimming velocities.

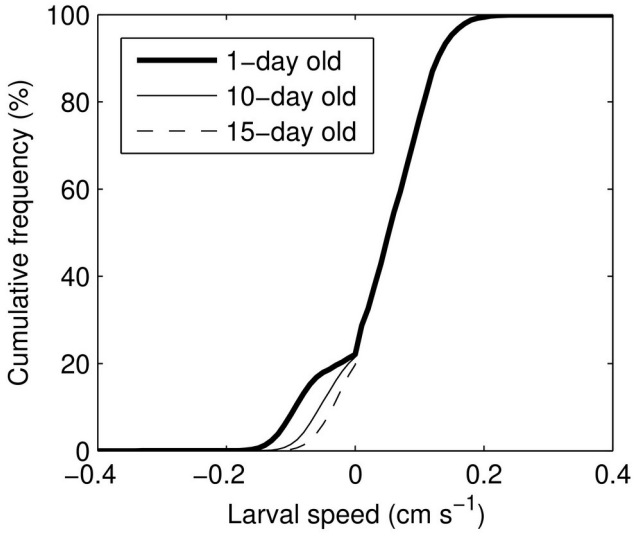

Fig. 4 Modeled cumulative frequency distribution of larval velocities on day 1 (solid line) and on day 15 (dashed line).

Online material

1. Deriving a motility behavior model for larval dispersal simulations from larval motility behavior experiments

Guizien et al. (2006) propose modeling larval dispersal by combining flow and larval velocities generated stochastically from a cumulative frequency distribution (CFD). The method of implementing larval velocities in a Lagrangian dispersal model (varying along tracks or in different tracks) will depend on the main source of variability in motility behavior (intra- or inter-individual). As larval velocity is expected to vary with age (due to ontogenic changes) and/or according to environmental conditions (i.e., light, depth or food) along the same track, intra-individual variability cannot be neglected. However, larval velocity may also vary as a result of different intrinsic abilities (bet-hedging hypothesis; Stearns 1976), but accounting for such variability is not necessary as long as it is lower than intra-individual variability.

Whatever the variability sources, larval velocity CFD used in the model should describe the larval motility behavior at sea, which could differ from that quantified in laboratory due to biases linked to two limitations: 1) duration of the experiments, and 2) size of the experimental containers.

As behavioral experiments are limited to durations of hours, intra- and inter-individual variability in swimming activity frequency cannot be separated: Although some larvae could display 100% activity during the experiment, it is unrealistic to extrapolate from this that 100% activity could be maintained over days. To avoid this bias, intra-individual larval velocity CFD is reconstructed from motility behavior experiments performed on a group of larvae by summing the swimming velocity CFD (computed on tracks of swimming larvae) weighted

by the swimming activity frequency, and the free drift velocity weighted by the swimming inactivity frequency (Fig. S1).

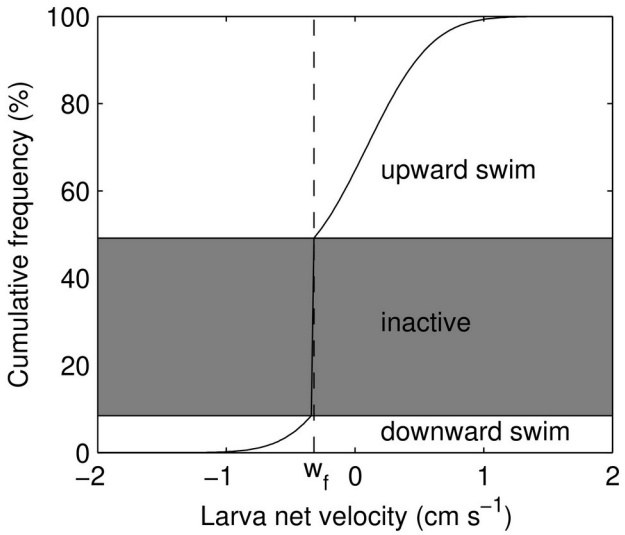

Fig. S1 Generic model of cumulative frequency distribution (CFD) of larval swimming velocities for negatively buoyant larvae: The grey area represents CFD during periods of inactivity characterized by free fall speed (dashed line). White areas represent CFD during upward and downward swim. W_f = free fall speed.

By definition, the sum of the activity and inactivity frequency is 1. Furthermore, in small-sized containers, directional drift (downward or upward) may lead to the accumulation of larvae either on the bottom or at the surface. In these cases, larvae escaping from tracking will be considered inactive, while the interpretation of the behavior depends on buoyancy. If negatively buoyant, for instance, larvae on the bottom of containers can reasonably be assumed to be free falling in an unbounded medium, while larvae at the surface should be considered upward swimming. Hence, larval velocity CFD at sea is a composite function reconstructed from experiments with unavoidable biases. In the case of negatively

buoyant larvae, this composite CFD is the weighted sum of three contributions and is written as:

$$CFD(age) = (A\ CFD_A(age) + B\ CFD_B(age) + C\ CFD_C(age))/(A+B+C) \quad (1)$$

where CFD_A is the free fall CFD, CFD_B is the net swim velocity CFD, CFD_C is the upward net swim velocity CFD for negatively buoyant larvae, A is the time the larvae spend on the bottom or free falling in the water column, B is the time spent in the water column not free falling, and C is the time spent at the free surface in the experimental containers.

2. Larval track reconstruction routine

Larval tracks were reconstructed from image sequences using a particle-tracking routine developed by the authors using the Matlab Image Processing toolbox. The main steps of the routine were as follows: for each frame, larvae were identified on the red plane component as white objects, contrasted from the background (applying a low-pass 2D filter over disks of 10 pixels in diameter). Larvae had a minimum body length of 6 pixels and a maximum surface of 90 pixels.^{2} Each larval track was then reconstructed from the nearest positions of two larvae in two successive frames. When this reconstruction was ambivalent concerning the presence in the frame of more than one larva near to another in the previous frame, the track was stopped and a new track started was for each larva. Larval tracks were scaled in pixels using an independent vial width for each film, yielding an average spatial resolution for position tracking of 0.017 cm pixel^{-1} on the horizontal and 0.012 cm pixel^{-1} on the vertical. A maximum vertical velocity threshold of 1.5 cm s^{-1} was applied, which exceeds the swimming capacity of red coral larvae.

3. Free fall speed measurements in flat-faced containers for free fall motion detection

To detect free fall motion along larval tracks, free fall velocities were measured in the same flat-faced containers used for swim video recordings to account for wall effects. The same procedure was applied as in the free fall velocity measurements in the large container. Larvae anesthetized with eugenol were gently injected into one vial one by one to minimize the movement caused by the injection itself and larval motion was recorded at 25 frames per second with a digital camera (SONY DCR-SR78); larval tracks were reconstructed applying the particle-tracking routine developed by the authors using the Matlab Image Processing toolbox (Online Material 1) to a sequence of frames sampled at a rate of 0.5 s. Vertical velocity components were computed along each recorded track and filtered out to detect uniform motion (when weight minus buoyancy equals drag) by removing accelerated or decelerated motion as result of the injection of the larvae or when the larvae were settling at the bottom of the containers. A larva was considered to be in uniform fall motion when the maximum deviation between the mean fall speeds during two consecutive periods of 2.5 s was lower than the standard deviation of the fall speed within the periods 2.5 s long. In most tracks, uniform fall motion was reached at a distance of 10 mm from the injection point and lasted at least 20 mm. The individual free fall speed and its precision were determined for each track, and hence larva, as the mean and standard deviation of the vertical speed during uniform fall motion. The correlation between age and sink speed was tested. If the correlation was significant, an 80% confidence interval around the linear regression best estimates was also calculated.

The larval free fall speed biased by wall effects in flat-faced containers displayed a large inter-individual variability, varying between -0.1 cm s^{-1} and -0.04 cm s^{-1} at all ages. Biased larval free fall velocities were significantly and positively correlated with age (t-test: $R^2 = 0.096$, $p < 0.0001$), increasing from X ± SD = -0.08 ± 0.026 cm s^{-1} on day 1 to -0.05 ± 0.026 cm s^{-1} on day 15, according to linear regression (Fig. S2).

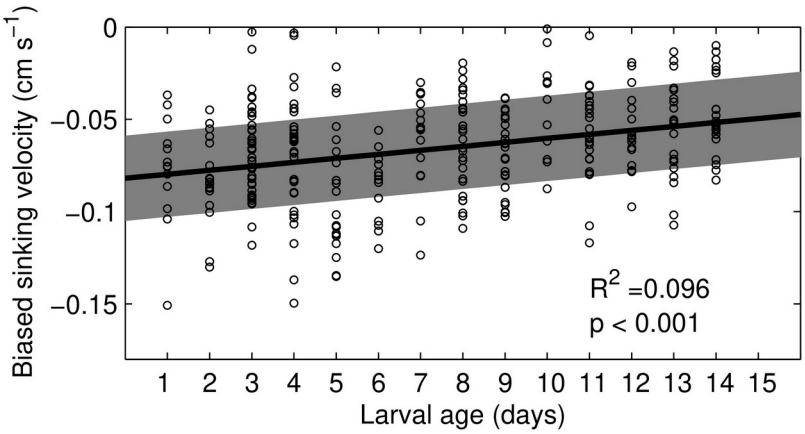

Fig. S2 Individual sinking velocities of *C. rubrum* larvae measured in a bounded flat-faced container during the first 15 days of PLD (hollow circles). Mean sinking velocities (solid line) and 80% confidence intervals around the mean (grey area) estimated from linear regression.